ASIAN JOURNAL OF PHARMACEUTICAL AND CLINICAL RESEARCH

INNOVARE ACADEMIC SCIENCES
Knowledge to Innovation

Vol 18, Issue 6, 2025

Online - 2455-3891
Print - 0974-2441

Research Article

PHYSICOCHEMICAL CHARACTERIZATION AND ANTIFUNGAL EFFICACY OF SILVER NANOPARTICLES AGAINST *CANDIDA* SPECIES

ARTI ZENDE[1], JAYANT PAWAR[1]*, CHITRA KHANWELKAR[2], ROHAN S PHATAK[3], PRIYANKA BIRLA[4], MANISH D SHINDE[4]

[1]Department of Biotechnology, Krishna Institute of Science and Technology, Krishna Vishwa Vidyapeeth (Deemed to be University), Karad, Maharashtra, India. [2]Department of Pharmacology, Krishna Institute of Medical Sciences, Krishna Vishwa Vidyapeeth (Deemed to be University), Karad, Maharashtra, India. [3]Department of Pharmacognosy, Krishna Institute of Pharmacy, Krishna Vishwa Vidyapeeth (Deemed to be University), Karad, Maharashtra, India. [4]Centre for Materials for Electronics Technology, Pune, Maharashtra India. *Corresponding author: Jayant Pawar; Email: jayantpawar26@gmail.com

Received: 06 March 2025, Revised and Accepted: 18 May 2025

ABSTRACT

Objective: This study aimed to evaluate the physicochemical properties of chemically synthesized silver nanoparticles (AgNPs) and assess their antifungal efficacy against *Candida* species.

Methods: AgNPs were synthesized using a co-precipitation method with silver nitrate and trisodium citrate and characterized via ultraviolet (UV)-Vis spectroscopy, X-ray diffraction (XRD), and field emission scanning electron microscopy (FE-SEM). Antifungal activity was determined using the broth microdilution method in 96-well plates. Cytoplasmic leakage assays and FE-SEM imaging were performed to understand the nanoparticles' mechanism of action.

Results: The UV-Vis spectrum showed a surface plasmon resonance peak at 410 nm, indicating nanoparticle formation with a band gap of ~3.03 eV. XRD confirmed a face-centered cubic crystalline structure, and FE-SEM revealed roughly spherical AgNPs (14.69–47.82 nm). The minimum inhibitory concentration was 15 µg/mL, whereas minimum fungicidal concentrations ranged from 125 to 500 µg/mL. Two-way analysis of variance ($p<0.001$) showed significant antifungal activity, with *C. albicans* being the most susceptible. Paired t-tests ($p<0.001$) confirmed significant cytoplasmic leakage in all species following AgNP exposure.

Conclusion: AgNPs demonstrated potent antifungal effects against *Candida* spp. by disrupting cell membranes. These findings support AgNPs as a promising alternative for managing VVC.

Keywords: Silver nanoparticles, *Candida* species, Antifungal activity, Vulvovaginal candidiasis, Co-precipitation method.

 DOI: http://dx.doi.org/10.22159/ajpcr.2025v18i6.54631. Journal homepage: https://innovareacademics.in/journals/index.php/ajpcr

INTRODUCTION

Vulvovaginal candidiasis (VVC) is a highly prevalent mucosal infection of the lower female reproductive tract, primarily caused by the opportunistic fungus *Candida albicans*. It accounts for about one-third of all vulvovaginitis cases in women of reproductive age, with approximately 70% of women experiencing at least one episode in their lifetime, and around 8% enduring recurrent infections [1-3]. The typical symptoms of VVC include vaginal itching, burning, pain, erythema, and often vaginal discharge, which is a mix of shed epithelial cells, immune cells, yeast, and vaginal secretions [4]. While 80–90% of VVC cases are attributed to *C. albicans*, the remaining cases are caused by other species like *Candida glabrata*, *Candida parapsilosis*, and *Candida tropicalis*.

The increasing prevalence of VVC in clinical practice is closely linked to the rising use of corticosteroids, broad-spectrum antibiotics, immunosuppressants, and the growing incidence of immunocompromising conditions like AIDS [5,6]. This makes effective treatment a significant concern in clinical settings. At presently, two primary classes of antifungal agents are used to manage VVC: polyenes and azoles. Polyenes, such as amphotericin B, are known for their potent antifungal effects but are also associated with considerable toxicity. On the other hand, azoles – including ketoconazole, fluconazole, and itraconazole – are more commonly used due to their broad antimicrobial activity and relatively safer profiles [6-9].

Among the various types of nanoparticles, inorganic nanoparticles have garnered significant attention due to their non-toxicity, hydrophilicity, biocompatibility, and high stability [10]. In recent years, nanotechnology has emerged as a promising field in medicine, particularly for its potential applications in drug delivery and antimicrobial therapies. Nanoparticles, with their ability to carry, stabilize, and protect therapeutic agents, offer a novel strategy for treating fungal infections like VVC. These particles can penetrate the extracellular polymeric substances surrounding fungal cells, allowing for more targeted and effective treatments, as evidenced in other eukaryotic cells [11,12]. Silver nanoparticles (AgNPs) have been particularly noted for their antimicrobial properties [13]. They interact with yeast cell membranes, disrupting the lipid bilayer and causing membrane pores that lead to ion leakage and cell death [14-16]. It was reported that AgNPs have also been shown to induce fungal cell death by generating reactive oxygen species (ROS), particularly hydroxyl radicals [14].

This study centers on three primary objectives: (1) synthesizing AgNPs using the co-precipitation method, (2) characterizing these synthesized nanoparticles, and (3) investigating their antifungal activity and mechanisms of action against *C. albicans* and non-albicans species such as *C. glabrata*, *C. tropicalis*, and *C. parapsilosis*. By exploring the potential of AgNPs as an alternative or adjunct therapy for VVC, this research aims to contribute to the development of more effective and targeted antifungal treatments.

METHODS

Synthesis of AgNPs

AgNPs were synthesized using the co-precipitation method as per the procedure of the previous study [17]. A 40 mL solution of 0.01 M silver nitrate ($AgNO_3$) was prepared and introduced into 100 mL of distilled water. The mixture was heated on a magnetic stirrer at 60°C for 2 min. Following this, 20 mL of a 0.01 M trisodium citrate solution was added, and the mixture was stirred for an additional 5 min until a milky white appearance indicated the onset of nanoparticle formation. To precipitate the nanoparticles, 100 mL of a 1 M sodium hydroxide (NaOH) solution was added dropwise, adjusting the pH to 14, which resulted in a color change to brown. The mixture was then stirred continuously for 16 h, yielding a grey-colored solution. The resulting solution was centrifuged and washed with distilled water to neutralize the pH. This was followed by further centrifugation in ethanol. The precipitate was dried at 80°C for 8 h to obtain a powdered form, which was then ground into fine particles using a mortar and pestle.

Characterization of AgNPs

The synthesized AgNPs were characterized using ultraviolet (UV)-Visible Spectroscopy to examine the optical properties of the nanoparticles. X-ray diffraction (XRD) used to analyze the crystal structure of the synthesized AgNPs. Field Emission Scanning Electron Microscopy with Energy Dispersive Spectroscopy (FESEM-EDS) determine the size and morphology of the nanoparticles.

Antifungal activity assessment

The antifungal activity of the synthesized AgNPs was tested against different *Candida* species associated with VVC, including *C. albicans*, *C. glabrata*, *C. tropicalis*, and *C. parapsilosis.* All cultures were procured from the National Collection of Industrial Microorganisms, Pune, and stored at refrigeration temperatures.

Qualitative determination of antifungal activity of AgNPs

The qualitative antifungal efficacy of AgNPs was evaluated using a broth microdilution assay in microtiter plates to determine their activity against *Candida* species. The *in vitro* fungicidal assay was conducted in a 96-well microtiter plate, with each well containing 200 µL of YPD broth supplemented with AgNPs at a concentration of 500 µg/mL and yeast cultures adjusted to a final cell density of 1×10^3 colony-forming unit (CFU)/mL. The plates were then incubated at 37°C±2°C for 48 h. Following incubation, the viable cell count method was used to assess yeast growth inhibition under a Neubauer chamber. Survival rates (CFU/mL) were determined relative to the untreated control, which was considered 100% survival.

Quantitative determination of antifungal efficacy of AgNPs

The quantitative antifungal activity of AgNPs was evaluated using a broth microdilution assay in microtiter plates to determine the minimum inhibitory concentration (MIC) and minimum fungicidal concentration (MFC). These values correspond to the lowest AgNP concentrations required to either inhibit yeast growth or achieve a 3-log reduction (99.9%) in viable yeast cells. Since the chemically synthesized AgNPs formed a suspension rather than a true solution in YPD medium, MFC values were determined by quantifying CFU/mL in a Neubauer chamber. The in vitro fungicidal assay was carried out in 96-well microtiter plates, where each well contained 200 µL of YPD broth supplemented with AgNPs at concentrations ranging from 15 µg to 1000 µg/mL, along with yeast cultures adjusted to a final density of 1×10^3 CFU/mL. The plates were incubated at 37°C±2°C for 48 h, after which yeast growth inhibition in each well was assessed through viable cell counting using a Neubauer chamber. The survival rates (CFU/mL) were calculated relative to the untreated control, which was considered 100% survival. The MIC was determined as the lowest AgNP concentration that visibly inhibited yeast growth [18,19].

Mode of action of AgNPs

To investigate the mode of action of AgNPs, against Candida spectroscopic analysis was performed to estimate the leakage of cytoplasmic contents from yeast cultures, including *C. albicans*, *C. tropicalis*, *C. parapsilosis*, and *C. glabrata*. Yeast cells were prepared at a concentration of approximately 1×10^5 CFU/mL and suspended in phosphate-buffered saline. The cells were then exposed to 500 µg/mL of AgNPs and incubated at 28°C±2°C for 6 h. Following incubation, the cultures were centrifuged to separate the cells, and the absorbance of the supernatant was measured at 260 nm using a UV-visible spectrophotometer to assess cytoplasmic leakage [14,15]. The percentage of cytoplasmic leakage was calculated using the following formula:

% Leakage = (Absorbance of treated cells − Absorbance of control/ Absorbance of treated cells) × 100

This study quantifies the extent of membrane damage caused by AgNPs, as cytoplasmic leakage is indicative of compromised membrane integrity.

Statistical analysis

Data were expressed as mean±standard deviation (SD) from three independent replicates (n=3). Two-way analysis of variance (ANOVA) was performed to evaluate the effects of AgNP concentration and *Candida* species on yeast viability, with significance set at $p<0.05$. Paired t-tests were used to compare absorbance values between untreated and AgNP-treated groups in the cytoplasmic leakage assay, with $p<0.001$ considered statistically significant.

RESULTS AND DISCUSSION

Synthesis of AgNPs

AgNPs were successfully synthesized using the co-precipitation method. Upon the addition of trisodium citrate, a brown precipitate was observed, which gradually turned gray after constant stirring for 16 hours. This indicated the reduction of silver ions and the formation of AgNPs. After washing and drying, a gray powder was obtained, yielding approximately 9 mg of product, which was subsequently used for further analysis.

Characterization of AgNPs

UV-visible spectroscopy analysis

UV-visible absorption spectrum of the AgNPs dispersed in distilled water revealed a sharp absorption edge at 410 nm **(**Fig. 1). This shift to a lower wavelength is characteristic of small AgNPs and can be attributed to the size quantization effect. The calculated band gap energy of the AgNPs was approximately 3.03 eV, which is higher than the bulk silver band gap value. This increase in band gap suggests that smaller particles with higher energy gaps may enhance their ability to disrupt cellular processes and generate ROS, contributing to their antifungal properties.

XRD analysis

The XRD pattern of the synthesized AgNPs confirmed the formation of a face-centered cubic structure of silver, as inferred from the JCPDS card number 03-065-8428 **(**Fig. 2). The presence of sharp and distinct peaks further validated the crystalline nature of the AgNPs.

FE-SEM and EDS analysis

FE-SEM analysis of AgNPs revealed a homogeneous particle distribution (Fig. 3a). The irregular, roughly spherical nanoparticles range in size from 14.69 nm to 47.82 nm, with some degree of aggregation. EDS confirmed the successful synthesis of high-purity AgNPs, with elemental mapping showing a uniform silver distribution across the sample. The EDS spectrum detected only silver, with no significant impurities, validating the purity of the synthesized nanoparticles (Fig. 3b).

Qualitative determination of antifungal activity of AgNPs

The quantitative assay confirms the potent antifungal properties of AgNPs, demonstrating varying susceptibility among *Candida* species. Fig 4, indicated that at a concentration of 500 µg/mL, the AgNPs exhibited significant antifungal activity against *Candida* spp. In the

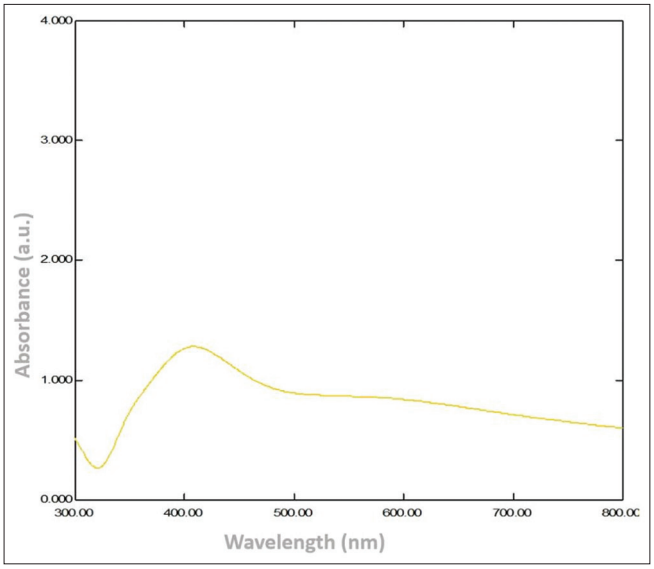

Fig. 1: Ultraviolet-visible absorption spectrum of silver nanoparticles (AgNPs). The characteristic surface plasmon resonance peak at 410 nm indicates the successful synthesis of AgNPs. The shift to a lower wavelength suggests the formation of small-sized nanoparticles, likely due to the size quantization effect

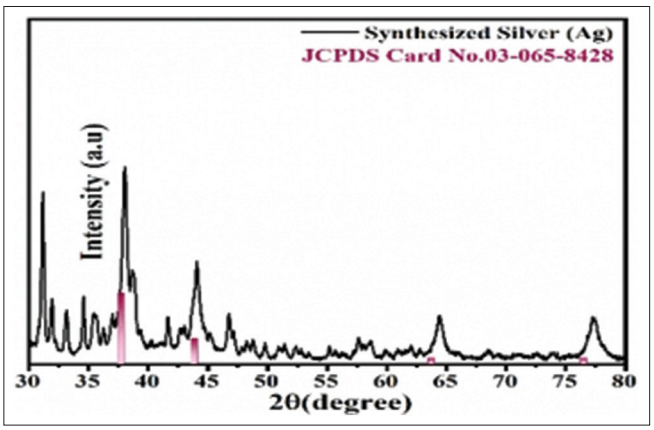

Fig. 2: X-ray diffraction pattern of silver nanoparticles confirms the formation of face-centered cubic structured silver nanoparticles, as referenced by JCPDS card number 03-065-8428. Sharp and distinct peaks further validate their crystalline nature

control group (without AgNP treatment), all *Candida* species exhibited high CFU counts, indicating normal fungal growth in the absence of AgNPs. However, upon treatment with 500 µg/mL of AgNPs, a significant reduction in CFU counts was observed across all species. *C. tropicalis* was completely inhibited, showing no detectable CFUs. *C. glabrata* exhibited a CFU count of 7.15×10^5, indicating a considerable reduction but higher resistance compared to other species. *C. parapsilosis* displayed 2.025×10^5 CFUs, suggesting strong susceptibility to AgNPs. Meanwhile, *C. albicans* demonstrated the lowest residual growth with 7.04×10^4 CFUs, highlighting its high sensitivity to AgNPs treatment.

These findings suggest that while AgNPs exhibit potent antifungal activity, different *Candida* species show varying degrees of susceptibility, with *C. tropicalis* being the most affected and *C. glabrata* showing relatively higher resistance.

Quantitative estimation of antifungal activity of AgNPs

The antifungal efficacy of AgNPs against *Candida* species was quantitatively assessed using the CFU count method. The results (Table 1 and Fig. 5) demonstrate a progressive decline in CFU count with increasing concentrations of AgNPs, indicating a dose-dependent antifungal effect. At 500 µg/mL, *C. tropicalis* was completely inhibited (CFU=0), while *C. glabrata*, *C. parapsilosis*, and *C. albicans* exhibited significant reductions in viability. Among these, *C. parapsilosis* and *C. albicans* demonstrated higher resistance at lower concentrations compared to *C. tropicalis*, as evident from their remaining CFU counts.

The MIC of AgNPs was determined to be 15 µg/mL, while the MFC ranged from 125 µg/mL to 500 µg/mL for all tested *Candida* species. Notably, concentrations below 15 µg/mL did not exhibit significant antifungal activity, reinforcing the threshold required for effective fungal inhibition. These findings are consistent with previous reports on the antimicrobial properties of AgNPs and their efficacy in disrupting fungal cell viability [20,21]. The spectroscopic analysis of cytoplasmic leakage further corroborated these results, suggesting that AgNPs exert their antifungal action by disrupting the yeast cell membrane, leading to cellular content leakage (Table 2). Collectively, these observations underscore the potential of AgNPs as a potent antifungal agent, with promising applications in antifungal therapeutics and infection control.

The antifungal efficacy of AgNPs against various *Candida* species was evaluated by a two-way ANOVA where AgNP concentration and species type considered as independent variables and CFU counts as the dependent variable, based on mean values assuming normal distribution and variance homogeneity. The results showed a highly significant main effect of AgNP concentration ($p<0.001$), indicating that higher concentrations of AgNPs significantly reduced CFU counts across all species, consistent with their known dose-dependent antimicrobial action. A significant main effect of species ($p<0.01$) was also observed, suggesting varying susceptibility, with *C. tropicalis* showing the highest sensitivity and complete CFU inhibition at 500 µg/mL, whereas *C. glabrata* demonstrated greater resistance. Moreover, the significant interaction between concentration and species ($p<0.05$) confirmed that the response to AgNPs varied among species, emphasizing the need for species-specific dosing strategies. Therefore, these findings highlight the potent antifungal activity of AgNPs and underscore the importance of considering both concentration and pathogen type for optimal therapeutic outcomes.

Mode of action of AgNPs

The antifungal mechanism of AgNPs against *Candida* species was investigated using spectroscopic analysis and FE-SEM. The spectroscopic analysis of cytoplasmic leakage validated this mode of action, demonstrating a substantial increase in absorbance at 260 nm for all *Candida* species following AgNPs exposure (Table 2). Among the tested species, *C. albicans* exhibited the highest cytoplasmic leakage (72.04%), followed by *C. parapsilosis* (70.00%) and *C. tropicalis* (67.82%). In contrast, *C. glabrata* showed the lowest leakage (67.40%), indicating a relatively higher resistance to AgNP-induced membrane disruption. These observations confirm that AgNPs compromise yeast cell membrane integrity, leading to the release of intracellular contents and cell death. A paired t-test was conducted to compare absorbance values between untreated and treated conditions for each species. The absorbance values for treated cells were significantly higher than those for control cells, indicating substantial cytoplasmic release in response to AgNP exposure. Statistical analysis by paired t-test ($p<0.001$) confirmed that the increase in absorbance (indicative of cytoplasmic leakage) was significant across all species, highlighting the potential of AgNPs as a potent antifungal agent that causes membrane disruption in a dose-dependent manner. The observed variation in leakage across species suggests that AgNPs may induce different levels of damage depending on the species' inherent resistance mechanisms or membrane composition.

FE-SEM images further revealed that *Candida* cells underwent complete structural destruction following treatment with AgNPs (Fig. 6). The nanoparticles disrupted the integrity of the fungal cell membrane, leading to the leakage of intracellular components and subsequent cell death. These findings suggest that the antifungal activity of AgNPs is

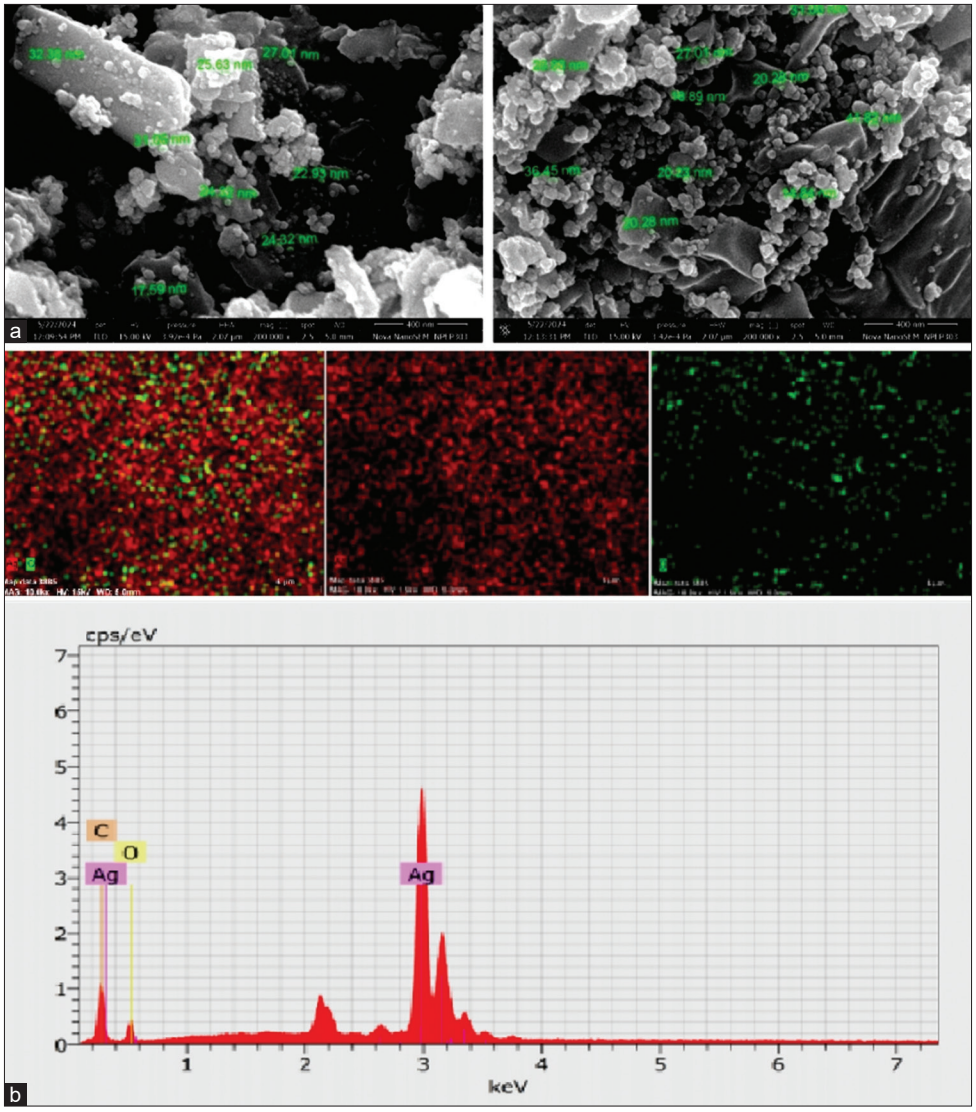

Fig. 3: (a) Field emission scanning electron microscopy of silver nanoparticles (AgNPs) revealed a uniform distribution of AgNPs and (b) Energy dispersive spectroscopy confirmed their high purity, showing only silver without detectable impurities. Elemental mapping further validated the even dispersion of silver across the sample

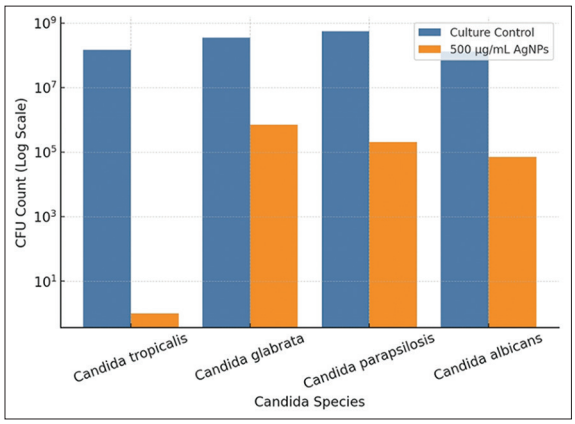

Fig. 4: Qualitative determination of antifungal efficacy of silver nanoparticles (AgNPs) against different *Candida* species using the microdilution and cell count method. At 500 µg/mL, AgNPs significantly inhibited Candida growth, reducing colony-forming unit (CFU) counts substantially. In contrast, the untreated control group showed high CFU counts, indicating normal fungal proliferation without AgNPs treatment

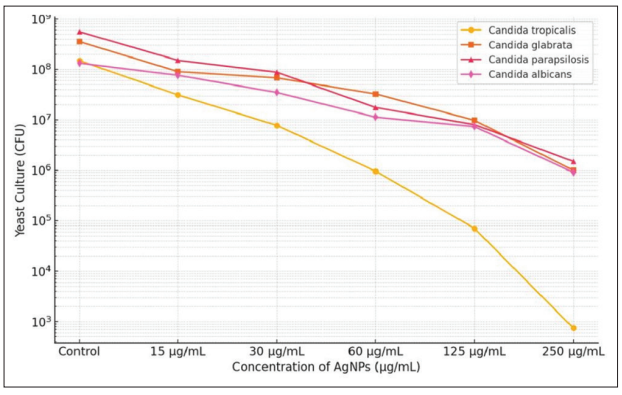

Fig. 5: Quantitative determination of antifungal efficacy of silver nanoparticles (AgNPs) against different *Candida* species using the colony-forming unit (CFU) count method. The plot reveals a dose-dependent reduction in CFU counts with increasing AgNP concentrations.

primarily mediated through membrane damage and oxidative stress, ultimately resulting in cell lysis.

Table 1: Quantitative determination of antifungal efficacy of AgNPs against *Candida* spp.

Yeast culture (CFU)/ Conc. of Ag NPs	*Candida tropicalis*	*Candida glabrata*	*Candida parapsilosis*	*Candida albicans*
Culture control	1.489×10^{8}	3.543×10^{8}	5.550×10^{8}	1.325×10^{8}
15 µg/mL	3.100×10^{7}	9.000×10^{7}	1.500×10^{8}	7.595×10^{7}
30 µg/mL	7.750×10^{6}	6.750×10^{7}	8.750×10^{7}	3.475×10^{7}
60 µg/mL	9.550×10^{5}	3.250×10^{7}	1.750×10^{7}	1.125×10^{7}
125 µg/mL	7.075×10^{4}	9.750×10^{6}	8.012×10^{6}	7.325×10^{6}
250 µg/mL	0.075×10^{4}	1.000×10^{6}	1.500×10^{6}	9.100×10^{5}
500 µg/mL	Nil	7.150×10^{5}	2.025×10^{5}	7.040×10^{4}

Data expressed as mean±SD; statistical analysis by two-way ANOVA (n=3) showed significant effects for AgNP concentration ($p<0.001$), *Candida* species ($p<0.01$), and a significant concentration-species interaction ($p<0.05$)

Table 2: Spectroscopic analysis of cytoplasmic leakage in yeast cultures treated with AgNPs

S. No.	Yeast speciesw	Absorbance recorded for control (Untreated)	Absorbance recorded for treated cells with 500 µg/mL AgNPs	Cytoplasmic leakage (%)
1	*Candida albicans*	0.052	0.186	72.04
2	*Candida tropicalis*	0.056	0.174	67.82
3	*Candida parapsilosis*	0.057	0.190	70.00
4	*Candida glabrata*	0.059	0.181	67.40

Data expressed as mean±SD; statistical analysis by paired t-test (n=3) showed significant cytoplasmic leakage in all species upon treatment with 500 µg/mL AgNPs ($p<0.001$)

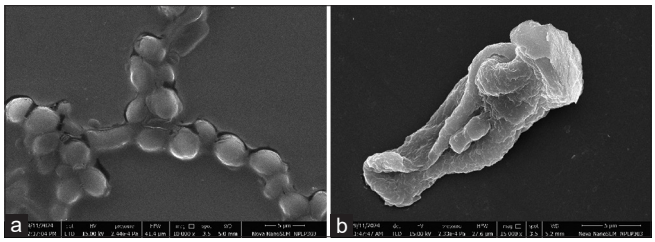

Fig. 6: Field emission scanning electron microscopy images of *Candida* species illustrating the cell structure. (a) Control (Untreated): Intact *Candida* cells with smooth, well-defined cell membranes, indicating normal cellular morphology. (b) Silver nanoparticle (AgNP)-Treated *Candida* cell: Significant structural damage is observed, including membrane disruption, surface irregularities, and complete cellular collapse, confirming the destructive impact of AgNPs on fungal cells

These results underscore the potent antifungal properties of AgNPs, reinforcing their potential as effective antifungal agents. The combination of structural damage, as evidenced by FESEM images, and increased cytoplasmic leakage, as shown by spectroscopic analysis, provides strong evidence that AgNPs disrupt fungal cell structures, making them promising *Candida*tes for antifungal therapeutics and infection control [22].

CONCLUSION

In this study, AgNPs were successfully synthesized using the co-precipitation method and characterized by various techniques, including UV-Vis spectroscopy, XRD, FE-SEM, and EDS. The results confirmed the formation of highly pure, crystalline AgNPs with a small particle size and high band gap energy, which enhanced their potential for antifungal activity. The synthesized AgNPs demonstrated significant antifungal efficacy against *C. albicans* and non-albicans species, such as *C. glabrata*, *C. tropicalis*, and *C. parapsilosis.* The MIC and MFC findings indicated that AgNPs could effectively inhibit fungal growth at relatively low concentrations. In addition, FESEM analysis revealed that AgNPs exert their antifungal effect by damaging the fungal cell membrane, leading to cellular disintegration and death.

Therefore, this study highlights the promising potential of AgNPs as a potent antifungal agent for the treatment of infections like VVC. Future studies should focus on optimizing the synthesis and exploring clinical applications of AgNP-based formulations for fungal infections.

AUTHORS' CONTRIBUTIONS

Conceptualization of the study: ArtiZende, JayantPawar, ChitraKhanwelkar; Study Design: JayantPawar; Experimental Work: ArtiZende, Priyanka Birla; Manuscript Preparation: ArtiZende, JayantPawar, Manish Shinde, RohanPhatak. All authors have read and approved the final manuscript.

CONFLICTS OF INTEREST

The authors declare no conflict of interest.

FUNDING

This research was supported by Maharashtra State Innovation Society (MSInS) and Krishna VishwaVidyapeeth (KVV), Karad under the Innovation and Research Promotion Scheme.

REFERENCES

1. Bairagi GR, Patel VP. Formulation and development of curcumin based emulgel in treatment and recurrence of vaginal candidiasis. Int J Curr Pharm Res. 2021;13(5):89-99. doi: 10.22159/ijcpr.2021v13i5.1900
2. Jeanmonod R, Chippa V, Jeanmonod D. Vaginal Candidiasis. Treasure Island, FL: StatPearls Publishing; 2025 Jan. Available from: https://www.ncbi.nlm.nih.gov/books/NBK459317
3. Farr A, Effendy I, Tirri BF, Hof H, Mayser P, Petricevic L, *et al.* Vulvovaginal candidosis (excluding mucocutaneous candidosis): guideline of the German (DGGG), Austrian (OEGGG) and Swiss (SGGG) society of gynecology and obstetrics (S2k-level, AWMF Registry Number 015/072, September 2020). Geburtshilfe Frauenheilkd. 2021;81(4):398-421. doi: 10.1055/a-1345-8793, PMID 33867561
4. Willems HM, Ahmed SS, Liu J, Xu Z, Peters BM. Vulvovaginal candidiasis: A current understanding and burning questions. J Fungi (Basel). 2020;6(1):27. doi: 10.3390/jof6010027, PMID 32106438
5. Rosati D, Bruno M, Jaeger M, Ten Oever J, Netea MG. Recurrent vulvovaginal candidiasis: An immunological perspective. Microorganisms. 2020;8(2):144. doi: 10.3390/microorganisms8020144, PMID 31972980
6. Disha T, Haque F. Prevalence and risk factors of vulvovaginal candidosis during pregnancy: A review. Infect Dis Obstet Gynecol. 2022;2022:6195712. doi: 10.1155/2022/6195712, PMID 35910510
7. Cui X, Wang L, Lü Y, Yue C. Development and research progress of anti-drug resistant fungal drugs. J Infect Public Health. 2022;15(9):986-1000. doi: 10.1016/j.jiph.2022.08.004, PMID 35981408
8. Souza CM, Bezerra BT, Mellon DA, de Oliveira HC. The evolution of antifungal therapy: Traditional agents, current challenges and future perspectives. Curr Res Microb Sci. 2025;8:100341. doi: 10.1016/j.crmicr.2025.100341, PMID 39897698
9. Pawar JR, Phatak RS, Qureshi NM, Singh AE, Shinde MD, Amalnerkar DP, *et al*. Contemporary trends in active and intelligent polymer nanocomposite based food packaging systems for food safety and sustainability in the modern aeon. Curr Mat Sci. 2024;17(4):e120723218668.
10. Abdel-Megeed RM. Biogenic nanoparticles as a promising drug delivery system. Toxicol Rep. 2025;14:101887. doi: 10.1016/j.toxrep.2024.101887, PMID 39867515.
11. Li B, Pan L, Zhang H, Xie L, Wang X, Shou J, *et al*. Recent developments on using nanomaterials to combat *Candida albicans.* Front Chem. 2021;9:813973. doi: 10.3389/fchem.2021.813973, PMID 35004630

12. Karna SR, Kavitha R, Damodharan N. Anticancer activity of silver nanoparticle of prodigiosin on lung cancer. Int J Appl Pharm. 2023;15(1):264-8. doi: 10.22159/ijap.2023v15i1.43628
13. More PR, Pandit S, Filippis AD, Franci G, Mijakovic I, Galdiero M. Silver nanoparticles: Bactericidal and mechanistic approach against drug resistant pathogens. Microorganisms. 2023;11(2):369. doi: 10.3390/microorganisms11020369, PMID 36838334
14. Mussin J, Giusiano G. Biogenic silver nanoparticles as antifungal agents. Front Chem. 2022;10:1023542. doi: 10.3389/fchem.2022.1023542, PMID 36277355
15. Abosede OO, Ezegwu LE. Synthesis and spectroscopic characterization of silver (I) mebendazole complexes. Int J Chem Res. 2022;6(2):1-5.
16. Gupta M. Inorganic nanoparticles: An alternative therapy to combat drug resistant infections. Int J Pharm Pharm Sci. 2021;13(8):20-31. doi: 10.22159/ijpps.2021v13i8.42643
17. Shirsat S, Pawar D, Jain N, Pawar J, Tale VS, Henry R. Synthesis of copper oxide nanoparticles by chemical precipitation method for the determination of antibacterial efficacy against *Streptococcus* sp. and *Staphylococcus* sp. Asian J Pharm Clin Res. 2019;12(5):135-8. doi: 10.22159/ajpcr.2019.v12i5.32270
18. Czernel G, Bloch D, Matwijczuk A, Cieśla J, Kędzierska-Matysek M, Florek M, *et al*. Biodirected synthesis of silver nanoparticles using aqueous honey solutions and evaluation of their antifungal activity against pathogenic *Candida* spp. Int J Mol Sci. 2021;22(14):7715. doi: 10.3390/ijms22147715, PMID 34299335
19. Pawar JS, Patil RH. Green synthesis of silver nanoparticles using *Eulophia herbacea* (Lindl.) tuber extract and evaluation of its biological and catalytic activity. SN Appl Sci. 2020;2(1):52. doi: 10.1007/s42452-019-1846-9
20. Bahey MG, Gabr BM, Gabr AM, Abo Hagar AM, Hegazy EE. Effect of silver nanoparticles on different *Candida* species isolated from patients with oral candidiasis. Microb Infect Dis. 2024;5(4):1642-53. doi: 10.21608/mid.2024.295446.1980
21. Naik LS, Ramana Devi CV. Phyto-fabricated silver nanoparticles inducing microbial cell death via reactive oxygen species-mediated membrane damage. IET Nanobiotechnol. 2021;15(5):492-504. doi: 10.1049/nbt2.12036, PMID 34694754
22. Robinson JR, Isikhuemhen OS, Anike FN, Subedi K. Physiological response of *Saccharomyces cerevisiae* to silver stress. J Fungi (Basel). 2022;8(5):539. doi: 10.3390/jof8050539, PMID 35628793